

# Stable nanobridge formation in $\langle 110 \rangle$ gold nanowires under tensile deformation

Harold S. Park<sup>a,\*</sup>, Jonathan A. Zimmerman<sup>b</sup>

<sup>a</sup> Department of Civil and Environmental Engineering, Vanderbilt University, VU Station B 351831, 2301 Vanderbilt Place, Nashville, TN 37235, United States

<sup>b</sup> Sandia National Laboratories, Livermore, CA 94551, United States

Received 6 October 2005; received in revised form 20 November 2005; accepted 23 November 2005

Available online 27 December 2005

## Abstract

We present atomistic simulations of  $\langle 110 \rangle$  oriented gold nanowires under tensile deformation. We find that  $\langle 110 \rangle$  gold nanowires tend to form elongated, stable nanobridges upon necking, which is in agreement with previous experimental observations. In addition, the simulations reveal that the formation of a high strength multishell lattice structure during the plastic deformation of the  $\langle 110 \rangle$  wires may account for the stability of the elongated nanobridges observed experimentally.

© 2005 Acta Materialia Inc. Published by Elsevier Ltd. All rights reserved.

**Keywords:** Gold nanowires; Atomistic simulations; Nanobridge; Stacking fault energy; Multishell lattice structure

## 1. Introduction

The understanding and functionalization of metallic nanowires has become a topic of major interest to the international materials science and engineering communities. The major reasons are due to the improved mechanical, electrical and optical properties that result from the small sizes of these materials [1,2]. For example, gold nanowires have been extensively studied for the past decade. This is mainly because gold nanowires are viewed as having enormous potential as interconnects in electrical applications, and also due to the availability of accurate interatomic potentials for studying the behavior of gold using molecular dynamics (MD) simulations.

Gold nanowires have also been shown experimentally to exhibit an orientational dependence on the mode of tensile failure. For example, the experiments of Kondo and Takanayagi [3] illustrated that  $\langle 110 \rangle$  oriented nanowires tend to form elongated, stable nanobridges during necking

which are as narrow as a few nanometers. In contrast,  $\langle 100 \rangle$  oriented gold nanowires were seen to form necked regions of disorder prior to fracture. Rodrigues et al. [4] also studied the elongation of  $\langle 100 \rangle$  and  $\langle 110 \rangle$  gold nanowires; they similarly found that  $\langle 110 \rangle$  nanowires tended to form elongated rod-like nanobridges with larger cross-sections than the atomic chains found during the elongation of  $\langle 100 \rangle$  gold nanowires.

Recent MD simulations have offered more evidence for the stability of  $\langle 110 \rangle$  nanowires. For example, the work of Gall et al. [5,6] has shown that initially  $\langle 100 \rangle$  gold nanowires may undergo a tetragonal phase transformation to a final body-centered tetragonal structure. Similarly, researchers have shown that face-centered cubic (fcc) nanowires spontaneously relax at finite temperature from initially  $\langle 100 \rangle$  oriented nanowires to  $\langle 110 \rangle$  oriented nanowires with  $\{111\}$  faces [7–10]. For certain materials, the reoriented  $\langle 110 \rangle / \{111\}$  wires were found to show both shape memory [7] and pseudoelastic behavior [7,9,10]. Theoretical support for these experimental findings was put forth by Jagla and Tosatti [11], in which Monte Carlo simulations driven by the minimization of surface energy were utilized to show that  $\langle 110 \rangle$  orientations were indeed

\* Corresponding author. Tel.: +1 615 936 7807; fax: +1 615 332 3365.  
E-mail address: [harold.park@vanderbilt.edu](mailto:harold.park@vanderbilt.edu) (H.S. Park).

energetically preferable for gold nanowires in the absence of surface diffusion. These findings indicate that nanowires created using a top-down methodology out of a bulk metal are not in a minimum energy configuration, and can reorient to the preferred  $\langle 110 \rangle$  orientation. While both first principles [12–14] and MD simulations of nanowire mechanical behavior have been performed [15–23], analysis of the effects of different orientations has been considered by few researchers [12,24].

Thus, the objective of this work is to use atomistic simulations to understand the tensile behavior of the preferred  $\langle 110 \rangle$  orientation for gold nanowires, and in particular to explain the stability of long, elongated nanobridges which emanate from  $\langle 110 \rangle$  gold nanowires. The key finding of this work is that the stability of the elongated nanobridges emanating from  $\langle 110 \rangle$  gold nanowires may be due to the presence of a high strength multishell lattice structure that forms as an outcome of the plastically deforming nanowire. In addition, the multishell lattice structure is found to be increasingly stable as the tensile strain rate is decreased, indicating the validity of such a hypothesis at the lower strain rates at which nanoscale experiments are generally performed.

## 2. Simulation methods

We performed MD simulations using the embedded-atom method (EAM) [25] as the underlying atomic interaction model. All simulations in this work were done using the EAM potential of Foiles [26], which was fit to the cohesive energy, equilibrium lattice constant, bulk modulus, cubic elastic constants and the unrelaxed vacancy formation energy, bond length and bond strength of the diatomic molecule. The Foiles potential was fit to essentially the same functional forms as used in the potential developed by Voter and Chen [27,28], with extra emphasis given to correctly modeling the stacking fault energy of gold. A full listing of the physical properties that characterize the

Foiles potential can be found in Park and Zimmerman [26], which also demonstrates the importance of correctly modeling stacking fault and surface energies in simulations of nanoscale plasticity.

Square cross-section gold  $\langle 110 \rangle$  nanowires were created out of a bulk fcc crystal. The wires were all 15 nm long, with varying cross-sectional lengths of 2.31 nm, 3.26 nm and 4.62 nm. The wires were first relaxed to an equilibrium minimum energy configuration with free boundaries everywhere, then thermally equilibrated to 300 K for 20 ps using a Nosé–Hoover thermostat [29,30] with a time step of 0.001 ps while keeping the length of the wires constant. The thermostat was removed prior to loading, ensuring adiabatic loading conditions; no periodic boundary conditions were utilized at any stage in the simulations.

The applied strain rates for each nanowire were  $3 \times 10^7 \text{ s}^{-1}$ ,  $3 \times 10^8 \text{ s}^{-1}$  and  $3 \times 10^9 \text{ s}^{-1}$  for each wire. The nanowires were loaded in tension in the  $\langle 110 \rangle$  direction by fixing one end of the wire, creating a ramp velocity profile which went from zero at the fixed end to a maximum value at the free end, then pulling the free end at the maximum value. The ramp velocity profile was utilized to avoid the emission of shock waves from the loading end of the wire. The equations of motion were integrated in time using a velocity Verlet algorithm, and all simulations were performed using the Sandia-developed code Warp [31–33].

## 3. Simulation results and discussion

Fig. 1 shows the deformation process of the 3.26 nm cross-section nanowire at a strain rate of  $\dot{\epsilon} = 3 \times 10^8 \text{ s}^{-1}$ . As can be seen, the nanowire loaded at this strain rate necks and forms a nanobridge which has a partial multishell structure; this is illustrated for the snapshot at  $t = 1935 \text{ ps}$ . Portions of the nanobridge are shown, in close-up, to the right of the deformed nanowire snapshots in Fig. 1, along with close-up views of the nanobridge cross-sections. By partial multishell structure, we mean a

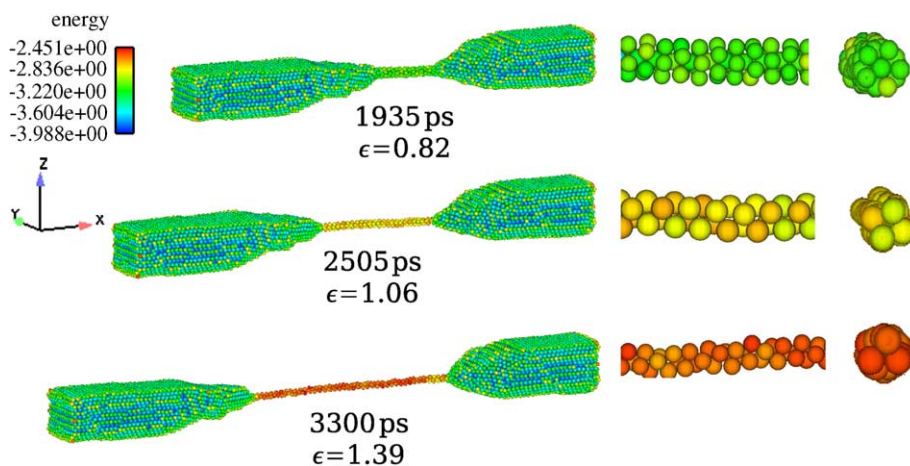


Fig. 1. Snapshots of the nanobridge deformation for the 3.26 nm wire at a strain rate of  $3 \times 10^8 \text{ s}^{-1}$ . Portions of the nanobridge are shown to the right of each nanowire configuration, followed by a cross-sectional snapshot of the nanobridge. The potential energy values are in eV.

structure comprised of a single chain of atoms surrounded by five nearest neighbors. However, because of the high loading rate, the nanobridge eventually reorients into a stabilized three atom thick chain (ATC) that is comprised of parallel  $\{111\}$  planes; this is seen in the  $t = 2505$  ps snapshot in Fig. 1. This reorientation has been observed for thin films experimentally by Kondo and Takanayagi [34], and numerically using MD simulations by Hasmy and Medina [35].

At even larger strains, the nanowire is unable to support the reoriented ATC structure and an unstable ATC forms ( $t = 3300$  ps in Fig. 1) in which atoms move in a helical, zig-zag pattern observed in first principles simulations by Sanchez-Portal et al. [13] and MD simulations by Park and Zimmerman [26]. The onset of the helical, zig-zag ATC indicates instability in the nanowire, and fracture occurs soon after.

To examine the effect of loading rate upon the stability of the nanobridge, we analyze the deformation process of

the 3.26 nm cross-section nanowire loaded at a lower strain rate of  $\dot{\epsilon} = 3 \times 10^7 \text{ s}^{-1}$ . As shown in Fig. 2, the initial multishell structured nanobridge elongates for a considerably longer period of time, and reaches a larger strain, before the loading rate overcomes the stable structure, again causing reorientation to the ATC. The multishell nanobridge reaches a length of about 9 nm before reorientation to the ATC occurs. At this reduced loading rate, the ATC elongates considerably before instability sets in, indicating that at even lower loading rates which are typically unattainable by MD simulation, the multishell structure could be expected to extend accordingly.

A close-up of the multishell structure observed during the deformation of the 3.26 nm cross-section gold nanowire loaded at a strain rate of  $\dot{\epsilon} = 3 \times 10^7 \text{ s}^{-1}$  is shown in Fig. 3. As can be seen, the structure of the nanobridge varies; the full multishell structure is observed in the bottom image of Fig. 3, which corresponds to the center of the nanobridge. The full multishell structure is characterized by a single

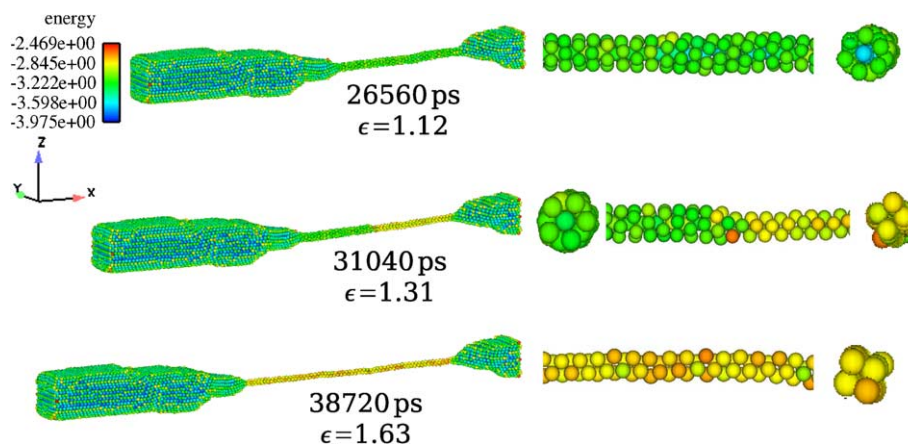


Fig. 2. Snapshots of the nanobridge deformation for the 3.26 nm wire at a strain rate of  $3 \times 10^7 \text{ s}^{-1}$ . Portions of the nanobridge are shown to the right of each nanowire configuration, followed by a cross-sectional snapshot of the nanobridge. The potential energy values are in eV.

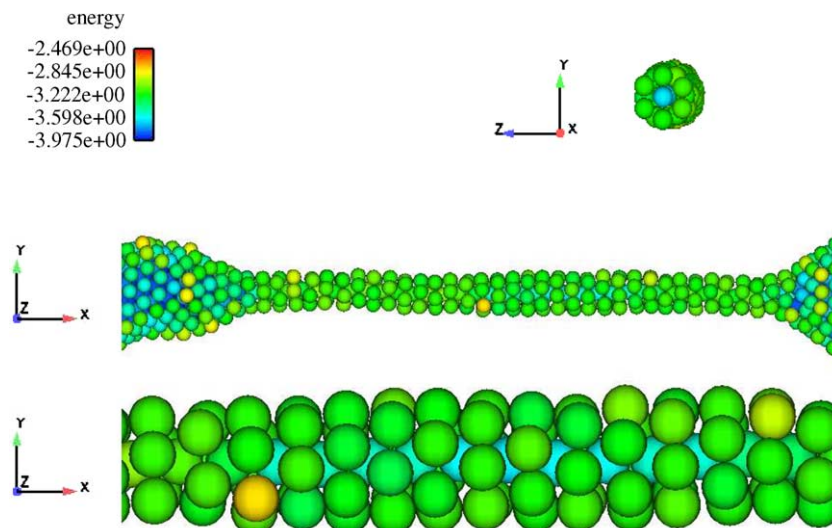


Fig. 3. Snapshots of the multishell nanobridge structure for the 3.26 nm wire at a strain rate of  $3 \times 10^7 \text{ s}^{-1}$ . The potential energy values are in eV.

atom chain that is essentially fully coordinated with six nearest neighbors within the  $yz$  plane. Near the ends of the nanobridge, the incomplete multishell structure is again observed in which the atom at the center has five nearest neighbors in the  $yz$  plane.

The existence of such multishell structures observed during the course of the nanowire deformation is significant, as it helps to explain the stability of the nanobridges observed in  $\langle 110 \rangle$  nanowires. Such multishell structures are extremely stable, as they represent an energetically favorable configuration in which surface area has been minimized [36]. This is best illustrated by comparing the potential energy values of the atoms in Figs. 1–3. In particular, Fig. 3 illustrates that the central atom of the multishell structure (the top snapshot in Fig. 3) is at a potential energy that is very close to that of an unstrained, bulk atom. Furthermore, even the neighboring atoms that surround the central atom in Fig. 3 have a lower energy than those atoms in the ATC configuration shown in Figs. 1 and 2.

The high strength of such multishell structures as compared to other nanowire geometries has been verified using MD simulations by Gall et al. [22]. However, the multishell nanowires considered in that work were idealized and created directly out of the bulk. In the present simulations, we have shown that the multishell lattice structure can be created due to the plastic deformation of an originally larger cross-section nanowire. Furthermore, while MD simulations typically operate at large strain rates that are not comparable to experimental findings, it is noteworthy that the tendency to form stable multishell structures increases as the loading rate decreases within the simulations shown here.

A relevant issue to consider are potentially anomalous thermal effects within the nanobridges. In Fig. 4, we show

snapshots of the kinetic energy within the elongating nanobridge for the 3.26 nm wire loaded at a strain rate of  $3 \times 10^9 \text{ s}^{-1}$ . We show kinetic energy per atom instead of temperature per atom due to inherent difficulties in defining temperature as a per atom quantity. This strain rate was chosen as it was the highest considered in this work, and would thus be the most likely to demonstrate any thermal irregularities in the nanobridge.

As can be seen, the kinetic energies of the atoms within the nanobridge are slightly higher than those outside the necked region. This is understandable as once the necking has begun, the atoms to the right of the neck (i.e. in the  $+x$ -direction in Fig. 4) relax as the neck and the loading end of the wire absorb the majority of the applied loading. However, as shown in the potential energy snapshots of the nanobridge structures at each time in Fig. 4, the nanobridges form with definitive structure, and show no signs of amorphization or melting; all instabilities result naturally from continued tensile loading causing eventual failure of the nanobridge. More importantly, the kinetic energies of the atoms within the nanobridge at the lower strain rates of  $3 \times 10^8 \text{ s}^{-1}$  and  $3 \times 10^7 \text{ s}^{-1}$  were not higher than for the atoms in the bulk, indicating a lack of anomalous thermal effects on the nanobridge formation and deformation.

The extensional lengths of the nanobridges prior to fracture as a function of nanowire size and loading rate are summarized in Fig. 5. The lengths of nanobridges that are formed in the tensile deformation of  $\langle 100 \rangle$  wires are shown for comparison. As can be seen in Fig. 5, with the exception of the 2.31 nm cross-section wire loaded at a strain rate of  $3 \times 10^8 \text{ s}^{-1}$ , the nanobridge length increased with decreasing loading rate for the initially  $\langle 110 \rangle$  oriented nanowires. Furthermore, the nanobridge length tends to decrease with increasing wire size with the exception of

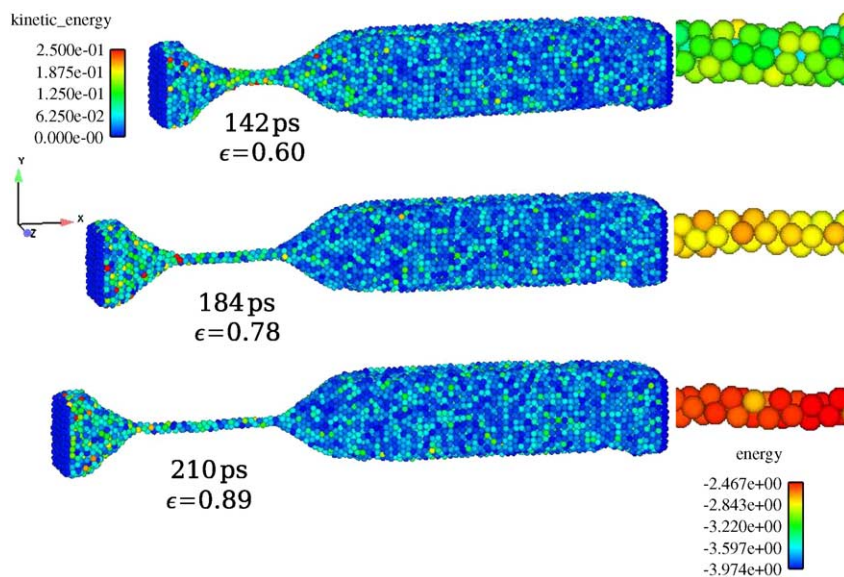


Fig. 4. Snapshots of the kinetic energy for the 3.26 nm wire at a strain rate of  $3 \times 10^9 \text{ s}^{-1}$ . Portions of the nanobridge are shown to the right of each nanowire configuration and atoms are colored according to values of potential energy in eV.

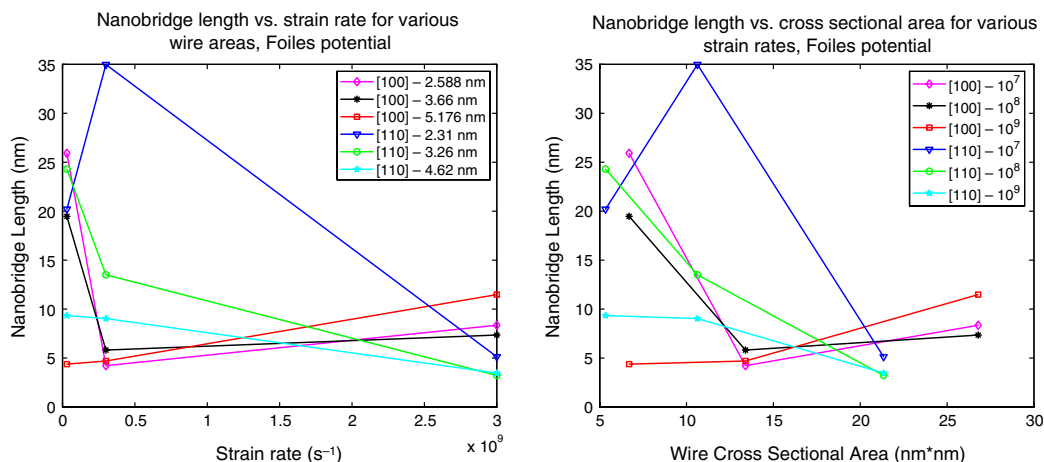


Fig. 5. Nanobridge length versus (left) strain rate and (right) cross-sectional area for various cross-sectional areas and both  $\langle 110 \rangle$  and  $\langle 100 \rangle$  orientations.

the 2.31 nm nanowire loaded at a strain rate of  $3 \times 10^7 \text{ s}^{-1}$ , which indicates that large surface-stresses [5] and side surface orientation [8] may play a significant role in the formation and stability of very low coordinated nanostructures such as nanobridges.

In contrast, it is difficult to ascertain a consistent trend in the length of nanobridges formed from initially  $\langle 100 \rangle$  oriented nanowires, as there appears to be no correlation between initial wire cross-sectional area and eventual nanobridge length. Moreover, there also appears to be no strong data indicating whether the nanobridge lengths tend to increase or decrease with decreasing strain rate. While relatively high strain rates across three orders of magnitude have been considered here, the trends are consistent with that observed experimentally, i.e. nanobridges formed from initially  $\langle 110 \rangle$  oriented gold nanowires are much more stable than the necked regions seen in initially  $\langle 100 \rangle$  oriented gold nanowires [3,4].

#### 4. Conclusions

In summary, we have shown that the experimentally observed [3,4] stability of nanobridges arising from the tensile deformation of  $\langle 110 \rangle$  gold nanowires can be explained by a multishell lattice structure that forms during the plastic deformation of the nanowires. In addition, the multishell structures were found to have an inherent stability that is dependent on the external loading rate applied to the nanowires. While the length of the nanobridges can be characterized as a function of loading rate and wire cross-sectional area, no such conclusions can be drawn for  $\langle 100 \rangle$  gold nanowires, which is again in agreement with previously published experimental data [3].

#### Acknowledgements

We would like to thank E. Dave Reedy and Neville R. Moody for their support of this research. We would also like to thank Stephen M. Foiles for his help with character-

izing the EAM potential and Gregory J. Wagner for his assistance with using the WARP code. Sandia is a multi-program laboratory operated by Sandia Corporation, a Lockheed Martin Company, for the United States Department of Energies National Nuclear Security Administration under contract DE-AC04-94AL85000.

#### References

- [1] Lieber CM. MRS Bull 2003;28(7):486–91.
- [2] Yang P. MRS Bull 2005;30(2):85–91.
- [3] Kondo Y, Takayanagi K. Phys Rev Lett 1997;79(18):3455–8.
- [4] Rodrigues V, Fuhrer T, Ugarte D. Phys Rev Lett 2000;85(19):4124–7.
- [5] Diao J, Gall K, Dunn ML. Nature Mater 2003;2(10):656–60.
- [6] Gall K, Diao J, Dunn ML, Haftel M, Bernstein N, Mehl MJ. J Eng Mater Technol 2005;127:417–22.
- [7] Park HS, Gall K, Zimmerman JA. Shape memory and pseudoelasticity in metal nanowires. Phys Rev Lett., in press.
- [8] Park HS, Gall K, Zimmerman JA. Deformation of FCC nanowires by twinning and slip. J Mech Phys Solids, submitted for publication.
- [9] Liang W, Zhou M. J Eng Mater Technol 2005;127(4):423–33.
- [10] Liang W, Zhou M, Ke F. Nano Lett 2005;5(10):2039–43.
- [11] Jagla EA, Tosatti E. Phys Rev B 2001;64:205412.
- [12] Mehrez H, Ciraci S. Phys Rev B 1997;56(19):12632–42.
- [13] Sanchez-Portal D, Artacho E, Junquera J, Ordejon P, Garcia A, Soler JM. Phys Rev Lett 1999;83(19):3884–7.
- [14] da Silva EZ, da Silva AJR, Fazzio A. Phys Rev Lett 2001;87(25):256102.
- [15] Ikeda H, Qi Y, Cagin T, Samwer K, Johnson WL, Goddard III WA. Phys Rev Lett 1999;82(14):2900–3.
- [16] Landman U, Luedtke WD, Burnham NA, Colton RJ. Science 1990;248:454–61.
- [17] Branicio PS, Rino JP. Phys Rev B 2000;62(24):16950–5.
- [18] Walsh P, Li W, Kalia RK, Nakano A, Vashista P, Saini S. Appl Phys Lett 2001;78(21):3328–30.
- [19] Kang J-W, Hwang H-J. Nanotechnology 2001;12:295–300.
- [20] Wu HA, Soh AK, Wang XX, Sun ZH. Key Eng Mater 2004;261–263:33–8.
- [21] Liang W, Zhou M. Proc of the Institution of Mechanical Engineers, Part C: J Mech Eng Sci 2004;218(6):599–606.
- [22] Gall K, Diao J, Dunn ML. Nano Lett 2004;4(12):2431–6.
- [23] Diao J, Gall K, Dunn ML. Nano Lett 2004;4(10):1863–7.
- [24] Coura PZ, Legoas SG, Moreira AS, Sato F, Rodrigues V, Dantas SO, et al. Nano Lett 2004;4(7):1187–91.
- [25] Daw MS, Baskes MI. Phys Rev B 1984;29(12):6443–53.

- [26] Park HS, Zimmerman JA. *Phys Rev B* 2005;72:054106.
- [27] Voter AF. Los Alamos Unclassified Technical Report, LA-UR 93-3901, 1993.
- [28] Voter AF, Chen SP. In: *Proc of Materials Research Society Symp*, 1987;82: p. 175–80.
- [29] Nosé S. *J Chem Phys* 1984;81:511–9.
- [30] Hoover WG. *Phys Rev A* 1985;31:1695–7.
- [31] Plimpton SJ. *J Comput Phys* 1995;117:1–19.
- [32] Warp. Available from: <http://www.cs.sandia.gov/~sjplimp/lammps.html>, 2005.
- [33] Horstemeyer MF, Hamilton JC, Thompson A, Baskes MI, Plimpton SJ, Daruka I, et al., Sandia Technical Report, SAND2001-8111, 2001.
- [34] Kondo Y, Ru Q, Takayanagi K. *Phys Rev Lett* 1999;82(4):751–4.
- [35] Hasmy A, Medina E. *Phys Rev Lett* 2002;88(9):096103.
- [36] Kondo Y, Takayanagi K. *Science* 2000;289:606–8.